Technical Sciences, 2020, 23(2), 131–142

UNIWERSYTET WARMIŃSKO-MAZURSKI W OLSZTYNIE

Quarterly peer-reviewed scientific journal
ISSN 1505-4675
e-ISSN 2083-4527
TECHNICAL SCIENCES
Homepage: www.uwm.edu.pl/techsci/

DOI: https://doi.org/10.31648/ts.5394

AN ANALYSIS OF A CYLINDRICAL CYCLONE SEPARATOR USED IN AIRCRAFT TURBINE ENGINES

***Tomasz Szwarc*[1], *Włodzimierz Wróblewski*[2], *Tomasz Borzęcki*[3]**

[1] ORCID: 0000-0002-0391-3353
Avio Polska sp. z o.o.
Bielsko-Biała

[2]ORCID: 0000-0002-3617-3515
Department of Power Engineering and Turbomachinery
Silesian University of Technology

[3] ORCID: 0000-0002-4226-7921
Avio Polska sp. z o.o.
Bielsko-Biała

Received 5 April 2020, accepted 2 July 2020, available online 7 July 2020.

K e y w o r d s: Multi-phase flows, air-oil separator, gas turbine, cyclone, volume of fluid method.

A b s t r a c t

Cyclone separators are commonly used in the oil system of aircraft gas turbine engines to separate air from oil. The major advantages of cyclone separators are simple structure and high reliability that eliminate the need for frequent inspections. The efficiency of a cyclone separator has a decisive impact on oil quality, which directly affects the efficiency of the oil system. The new generation of engines requires more compact separator designs to reduce weight and minimize project costs while maintaining (and often increasing) an engine's efficiency and reliability. To meet these requirements and optimize the separator structure, the flow of the air-oil mixture has to be modeled in the design process. The aim of this study was to present a numerical simulation of an aircraft turbine separator with the use of the volume of the fluid model.

Correspondence: Tomasz Szwarc, Avio Polska sp. z o. o. ul. Grażyńskiego 141, 43-300 Bielsko-Biała, e-mail: tomasz.szwarc@avioaero.it

Introduction

A cyclone separator is a component installed inside the main engine oil tank (Fig. 1). The major advantage of a cyclone separator is its simple structure which does not require maintenance or frequent inspections. A cyclone separator separates air from oil. The air-oil mixture is generated during the lubrication process inside engines, bearings, sumps and gearbox cavities. A separator's efficiency has a decisive impact on oil quality, and it directly affects the efficiency of the oil system. Increased air content in oil decreases pressure in the system and induces higher-pressure fluctuations, which in turn affects improper lubrication and cooling of engine components (bearings, gears, splines, accessories). Aircraft cyclone separators have to meet many more requirements than typical industrial cyclone separators. Varied operating conditions during flight missions cause changes in parameters such as the air/oil ratio, oil tank level, pressure, attitude and position. High swirling flow inside the separator is frequently encountered, and it is not stable. Unstable distribution of the flow field determines separation performance.

This paper analyzes a numerical model of an air-oil separator under a single operating condition. The flow field in the separator is complex, and swirling and anisotropy phenomena are sometimes taken into consideration in the relevant analyses. According to some authors (CHANG 2016, DELGADILLO 2005, ESCUE 2010, GAO 2012, RUDOLF 2013, WANG 2015), the Reynolds Stress Model (RSM) or the Large Eddy Simulation (LES) technique should be applied, but these advanced models are not suitable for developing optimization algorithms in future investigations. The above models are time-consuming and quite challenging in terms of the required calculation hardware. In the industrial approach, two equation models are more commonly used (SZWARC 2019). The RNG k-ε model with a swirling option was applied in this study. The model can recreate the flow characteristics of a cyclone separator, which can be useful for designing and optimizing this engine component (WANG 2010). The impact of different turbulence models on the solution will be studied in the future. In the presented preliminary analysis, turbulence was modeled with the two equation RNG k-ε model that speeds up calculations (WANG 2010) (two equations vs. seven equations in the RSM). Two-phase flow was simulated with the volume of the fluid model. This model accounts for the free surface effect (HIRT 1981) in the oil tank, which also considerably influences the separator's performance (KRISTOFFERSEN 2017). Gas-liquid separators (e.g. ARPANDI 1996, ERDAL 1998, KRISTOFFERSEN 2017) and other aircraft engineering applications (e.g. EASTWICK 2006, FILIPPONE 2010) have been widely studied and discussed, but there is a general scarcity of research into cyclone separators in an aircraft engine oil system. The typical cases reported in the literature involve cyclone separators for the oil and gas industry which have a different geometry or air/oil ratio and are difficult

to compare with aircraft applications. Other publications describe cyclone separators with a similar geometry to that analyzed in this paper (CHANG 2016, RUDOLF 2013), but those devices are used in the mineral industry with different fluid types or fluid and solid mixtures.

The aim of this study was to analyze a numerical model of two-phase fluid flow. The main goal was to develop a numerical model for implementation in the optimization procedure. The results were used to formulate recommendations for designers of air-oil separators.

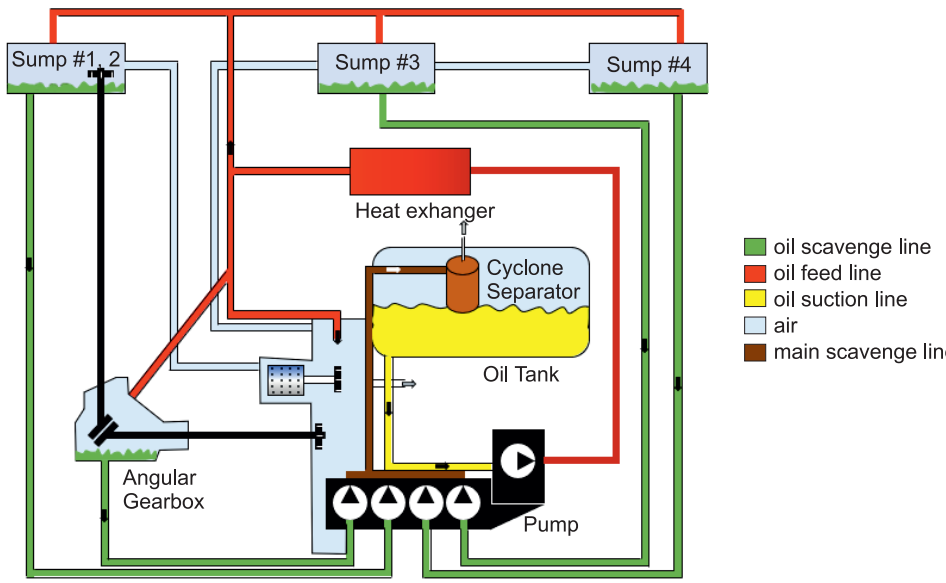

Fig. 1. Simplified scheme of an aircraft oil system

Oil lubricates and cools the components of a gas turbine engine, including bearings, gears, spline joints and dynamic seals. In the lubrication process, oil is aerated in sumps and gearboxes. The force of gravity drives oil to the lower parts of the engine where it is taken up by the scavenge pump and directed to the oil tank. The efficiency of the oil separator has a decisive impact on oil quality. A decrease in its parameters affects the operation of lubrication and cooling circuits. The optimal two-phase model has to be selected in analyses of computational fluid dynamics (CFD). The choice of the appropriate mathematical model depends on the type of flow at the separator inlet. This is a crucial requirement for simulating separation processes. A preliminary selection can be made based on two-phase flow maps (SZWARC 2019).

Numerical model

Geometry and boundary conditions

The geometry of the calculation domain was created based on the geometry of the test bench where a separator was installed in a cylindrical tank shown in Figure 2. The air-oil mixture flowed into the tank tangentially, and a swirl was generated inside the separator. Oil was directed towards the walls, and it flowed down into the tank. The separator had two outlets: one in the upper part and one at the bottom. Air was extracted from the separator through the upper outlet, and the presumably clear oil flowed through the bottom outlet. At the inlet, the mass flow rates of both air and oil were applied as boundary conditions. Uniform velocity with normal direction to the inflow cross-section was assumed. The mixture had constant temperature. Pressure conditions were specified at the outlets.

The experimental data were used to develop the simulation model. The test bench supports measurements of the inlet mass flow rate of each fraction at the inlet and the outlet, whereas pressure and temperature are measured only at selected points. Oil quality defined by Equation 1 was measured at the outlet

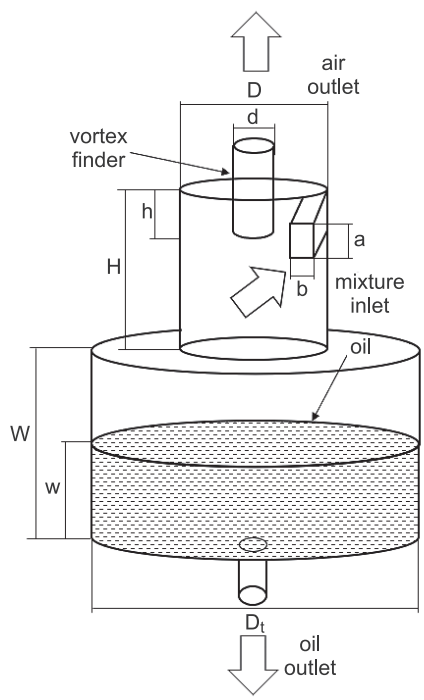

Fig. 2. A separator with the test tank

line by checking the volume fraction of each phase. Standard aviation oil for gas turbine engines was applied in the simulations. The volumetric air/oil ratio was 1.3 at the inlet. Numerical schemes for the analysis were selected based on the results reported by (WANG 2015). A coupled scheme with a pseudo transient option was selected as the solution algorithm for pressure-velocity coupling. For the preliminary numerical analysis, first-order upwind schemes were set for turbulent kinematic energy and the dissipation rate.

The boundary conditions at the outlets which enabled the determination of the prevailing conditions in the test stand were identified. The aim of the calculations was to determine separator performance which was described by two coefficients. The first coefficient denoted the amount of gas flowing through the oil outlet, whereas the second coefficient indicated the amount of oil flowing through the air outlet. These values were measured during the experiment. The oil quality coefficient (OQ) was defined as the volume fraction of oil at the oil outlet:

$$OQ = \left(\frac{\dot{V}_o}{\dot{V}_a + \dot{V}_o}\right)_{\text{oil outlet}} \tag{1}$$

Separation efficiency η_s was defined as the ratio of the difference between the volume rate of oil at the inlet and the volume flow rate at the outlet to the volume rate of oil at the inlet:

$$\eta_s = \frac{\dot{V}_{\text{o,inlet}} - \dot{V}_{\text{o,vent}}}{\dot{V}_{\text{o,inlet}}} \tag{2}$$

The determination of the optimal boundary conditions is a major challenge in the simulation process. Since air and oil masses were measured and mixed before entering the separator, the mass flow rate with a homogeneous distribution of the second phase was selected.

Pressure values were determined at both oil and air outlets. These boundary conditions are set to control the separation process. Other possible types of boundary conditions which are based on mass flow could not be applied at the outlets because the mass flow rates should be determined in a computational analysis. The dimensions of the test bench are presented in the Table 1.

Table 1

Dimensions of a cyclone with a tangential inlet

Dimensions	Cyclone height (H)	Vortex finder height (h)	Cyclone diameter (D)	Vortex finder diameter (d)	Inlet tube height (a)	Inlet tube width (b)	Tank height (W)	Tank diam. (D_t)
Parameter value (a)	3.2	1.4	3.6	1.3	1	1.6	12	3

Mathematical model of two-phase flow

The separation phenomena in an air-oil mixture are simulated with the Volume of the Fluid (*VoF*) model. This model supports tracking of the air-oil interface. The *VoF* is used to model the flow of two immiscible fluids. The following continuity equation is solved:

$$\frac{\partial}{\partial t}(\rho) + \nabla \cdot (\rho \vec{v}) = 0 \tag{3}$$

where:

$\vec{v}$ – the velocity vector,

ρ – the mixture density calculated from:

$$\rho = \alpha_a \rho_a + (1 - \alpha_a)\rho_o \tag{4}$$

where:

ρ_a – air density,

ρ_o – is oil density,

α_a – is the volume fraction of air which, in this case, represents the second phase.

The interface between the phases is tracked with a continuity equation for the volume fraction of air:

$$\frac{\partial}{\partial t}(\alpha_a \rho_a) + \nabla \cdot (\alpha_a \rho_a \vec{v}_a) = \dot{m}_{oa} - \dot{m}_{ao} \tag{5}$$

where:

$\dot{m}_{oa}$, $\dot{m}_{ao}$ are the mass flow rates from oil to air and air to oil, respectively.

The volume fraction equation is not solved for the oil phase (primary). The oil-phase volume fraction is computed based on the following constraint:

$$\alpha_a + \alpha_o = 1 \tag{6}$$

In this case, the volume fraction equation is solved with an implicit formula. A single momentum equation is solved for the entire domain, and the resulting velocity field is shared by the phases. The momentum equation 7 is dependent on the volume fractions of all phases, including mixture density ρ and mixture viscosity μ (UBBINK 1997):

$$\frac{\partial}{\partial t}(\rho \vec{v}) + \nabla \cdot (\rho \vec{v} \vec{v}) = -\nabla p + \nabla \cdot \left[\mu_{eff}(\nabla \vec{v} + \nabla \vec{v}^T)\right] + \rho \vec{g} + \vec{F} \tag{7}$$

where:

$\mu_{eff} = \mu + \mu_t$ – dynamic effective viscosity,

$\vec{g}$ – gravitational acceleration,

p – pressure,

$\vec{F}$ – the surface tension source term.

Turbulence

The RNG k–ε model is derived from the instantaneous Navier–Stokes equations using a mathematical technique known as "renormalization group" (RNG) methods. This technique is based on the standard k-ε model with some refinements. An additional term in the ε equation improves accuracy for rapidly strained flows. As a result, the effect of swirl on turbulence is taken into account, which improves the accuracy of swirling flows. The RNG theory provides an analytical formula for turbulent Prandtl numbers, whereas the standard k-ε model uses user-specified, constant values (YAKHOT 1986).

The following equations for turbulence kinetic energy k and dissipation rate of turbulent kinetic energy are solved:

$$\frac{\partial}{\partial t}(\rho k) + \frac{\partial}{\partial x_i}(\rho k U_i) = \frac{\partial}{\partial x_j}\left(\alpha_k \mu_t \frac{\partial k}{\partial x_j}\right) + G_k + G_b - \rho\varepsilon - Y_M + S_k \tag{8}$$

$$\frac{\partial}{\partial t}(\rho \varepsilon) + \frac{\partial}{\partial x_i}(\rho \varepsilon U_i) = \frac{\partial}{\partial x_j}\left(\alpha_\varepsilon \mu_t \frac{\partial \varepsilon}{\partial x_j}\right) + C_{1\varepsilon}\frac{\varepsilon}{k}G_k - C_{2\varepsilon}\rho\frac{\varepsilon^2}{k} - R_\varepsilon \tag{9}$$

where:

α_k and α_ε – the inverse effective Prandtl numbers for k and ε,

$C_{1\varepsilon}$ and $C_{2\varepsilon}$ – constant values of 1.42 and 1.68.

The scale elimination procedure in the RNG theory produces a differential equation for turbulent viscosity. Effective viscosity μ_t for the limit of very large Reynolds numbers is given by:

$$\mu_t = \rho C_\mu \frac{k^2}{\varepsilon} \tag{10}$$

where the value of C_μ = 0.0837 is derived with the RNG theory. Interestingly, the value of C_μ = is very close to the empirically determined value of 0.09 in the standard k-ε model (YAKHOT 1986).

Mesh

Separator geometry was divided into a tetra mesh generated with the Ansys Workbench tool 19.2. 3D geometry was meshed using a different number of elements, ranging from 512,000 to 1,527,000 tetra cells. The mesh was refined mainly in the regions close to the wall, and a moderate refinement was introduced in the central part of the separator domain. The quality of all 3D computational meshes with a different number of elements was checked before the simulation (see Tab. 2). Figures 3 and 4 show selected mesh overview.

Table 2

Mesh quality

Key factor	Requirement	Mean mesh quality
Aspect ratio	5:1	5.34
Orthogonal quality	>0.01 (best cell closer to 1)	0.96
Skew	below 0.95	0.82

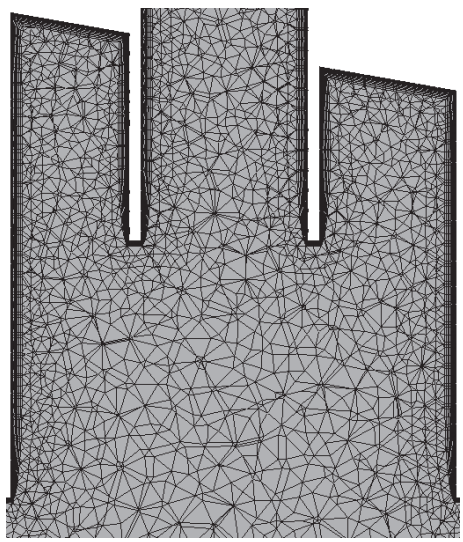

Fig. 3. Mesh at the cross-section of the separator

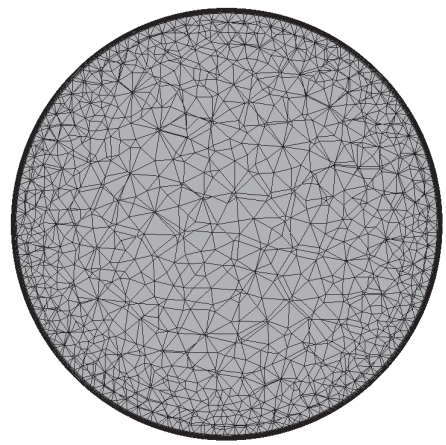

Fig. 4. Mesh at the bottom outlet of the separator

An analysis of the results of the first coarse mesh revealed satisfactory *OQ* values, but very low stability of the solution. A mesh independence analysis was performed to determine the impact of the size of the numerical grid. Two parameters were considered to guarantee the stability of the analysis: air and oil mass imbalance. An imbalance is defined as the sum of mass flows (inlet mass flow – outlet mass flows). The amplitude of the air mass flow rate at the outlet, oil quality and oil volume in the domain were selected to determine the influence of the mesh on the analyzed parameters. The results are presented in Figure 5. An increase in mesh density did not exert a significant influence on oil quality (the maximum difference was 13%). The oil level inside the domain remained stable. An improvement was observed in the parameters related to the stability of analysis. Considering *OQ* as the only goal of analysis, the mesh independence analysis demonstrated that changes in mesh refinement were relatively small. Lower density would significantly contribute to the optimization process.

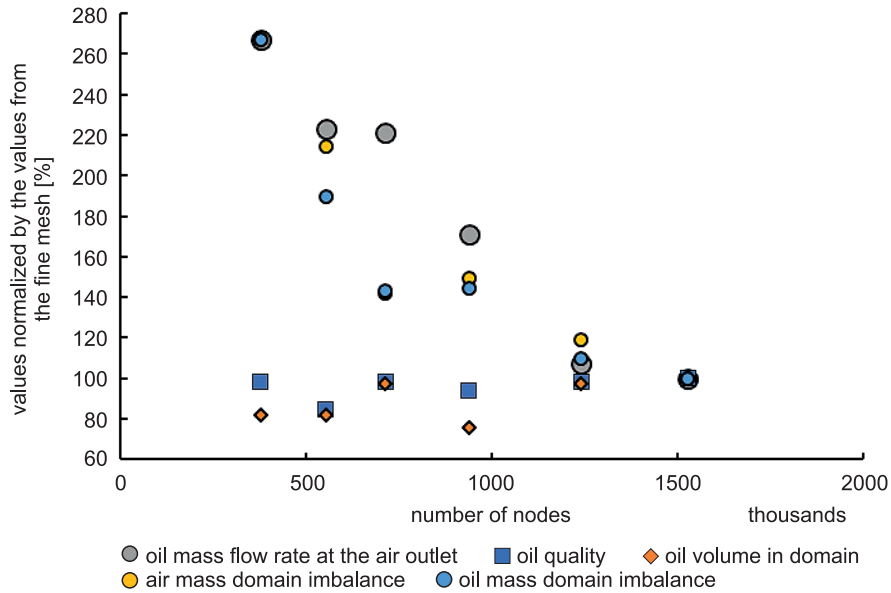

Fig. 5. Normalized solution parameters vs. the number of nodes

When the appropriate mesh type and density have been selected, the separator's geometry is optimized in the next step. Therefore, the selected mesh with 124k tetra cells guarantees the acceptable accuracy of the results and reasonable calculation time. This is an important consideration because a single case takes 1-2 weeks to compute with a computer cluster.

Calculation results

The aim of this study was to propose a numerical approach to an analysis of a cyclone separator. Oil was the primary phase, and air was the secondary phase. The analytical process became complicated already at the stage of formulating the initial conditions. The definition of initial values was a very important step in the calculations. Incorrect initial values lead to convergence problems or solver crash. Incorrect inlet pressure creates reverse flow at both outlets, which affects solver convergence and leads to mass imbalance problems. Inlet pressure was set based on the experimentally determined pressure drop in the separator. The preliminary simulation involved a very coarse mesh to determine the optimal working conditions. The analysis was initialized with an empty tank which was filled until the achievement of a stable oil level. The solver crashed when the simulation was initialized with a filled tank (Figs. 6, 7, 8, 9).

The location of the free surface in the oil tank is very sensitive to boundary conditions. This is an important factor which directly affects the formation of flow structures in the separator and, consequently, the separator's efficiency as predicted by (KRISTOFFERSEN 2017). This is a characteristic feature of open separators where the shape of the tank and oil level can impact performance. The main flow swirl in the cylinder causes oil separation, and oil is deposited on the separator wall. The main flow consisted of two phases. In the first phase, flow was parallel to the separator outlet, and in the second phase, flow occurred down the cylinder, creating a helical shape of streamlines (7 and 9). First-phase flow led to the accumulation of oil in the top corner of the separator, which is unlikely to occur due to recirculation with the incoming mixture. The second oil stream entering the tank influenced the oil free-surface.

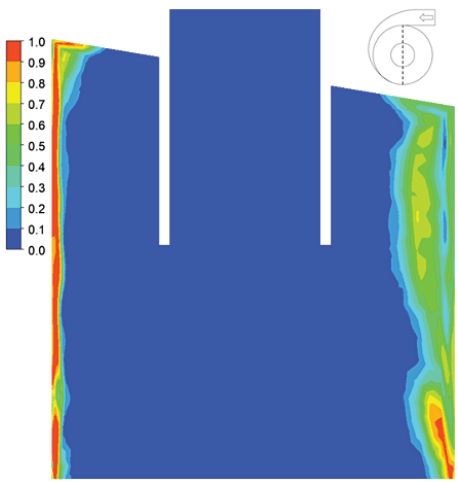

Fig. 6. Contour of the oil volume faction

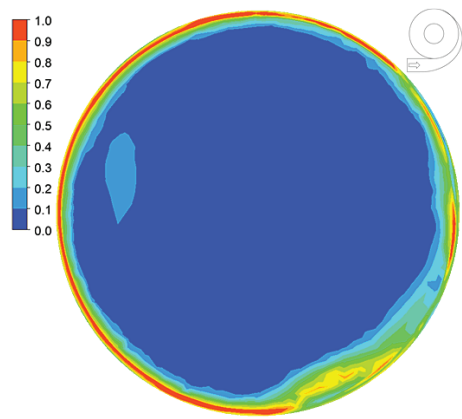

Fig. 7. Contour of the oil volume faction (bottom outlet of the separator)

The formation of oil film on the left wall is visible in Figure 6. The geometry of the inlet to the separation zone has a key impact on separation phenomena because it can rupture the formed film (Fig. 7). The axis of the vortex finder tube is not coincident with the outer diameter of the separator, which affects the formation of the inner swirl that flows directly to the vortex finder tube. The influence of the key geometrical features on flow structure will be investigated in the future after the numerical model has been validated.

The velocity distributions in the separator are visualized in Figure 8 and 9. The presented values were normalized by the values of average velocity at the cyclone inlet. Areas of both very low speed in the center of the separator (0-0.3) and high speed close to the walls (3-3.3) were observed.

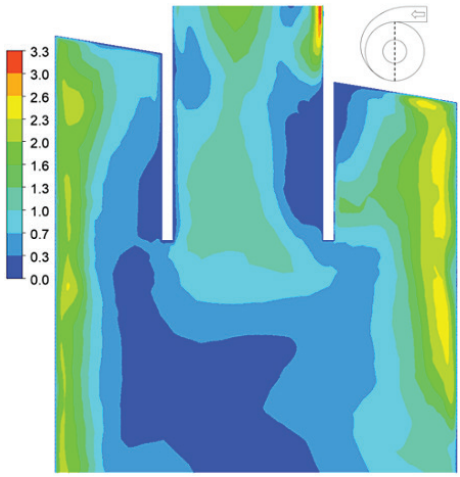

Fig. 8. Velocity contour

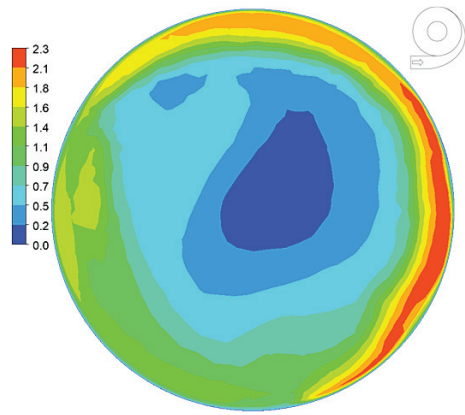

Fig. 9. Velocity contour(bottom outlet of the separator)

Table 3

Comparison of simulation results with test bench results

Parameter	Simulation results	Difference to test results
Normalized oil quality [%]	93.8	6.2
Normalized separation efficiency [%]	99.95	0.05

The experimentally determined values of oil quality OQ and separation efficiency η_s were compared with the results of numerical simulations. The difference in normalized oil quality reached 6.2% and in separation efficiency – 0.05% (Tab. 3). The resulting accuracy is satisfactory.

Conclusions

A cyclone separator was analyzed with the use of the presented calculation scheme. The *VoF* model was characterized by acceptable accuracy, and it offered a consensus between accuracy, robustness and modeling time. The selected boundary conditions stabilized oil volume inside the separator. The calculated pressure decrease was comparable with the experimentally determined pressure drop. The RNG k-ε model revealed a swirl structure inside the core of the separator. As expected, the results of the calculations indicate that oil level in the tank influences flow formation inside the separator. The separator inlet impacts the formation of the oil fraction close to the wall as well as its interaction with the free surface of the oil inside the tank. The observed changes in flow

parameters indicate that flow field was unsteady inside the separator. The above was confirmed by the mass flow rate of oil shown in Figure 5. Preliminary results demonstrated satisfactory alignment between the modeled results and the experimentally derived values. The results of the calculations for different experimental conditions will be analyzed in the future.

References

ARPANDI I., JOSHI A.R., SHOHAM O., SHIRAZI S., KOUBA G.E. 1996. *Hydrodynamics of two-phase flow in gas-liquid cylindrical cyclone separators*. Society of Petroleum Engineers, 1: 427–436, doi: 10.2118/30683-PA.

CHANG P., HU T., WANG L., CHANG S, WANG T., WANG Y. 2016. *Numerical simulation on structure optimization of liquid-gas cylindrical cyclone separator*. International Journal of Chemical Engineering, 3187631, doi: 10.1155/2016/3187631.

DELGADILLO J.A., RAJAMANI R.K. 2005. *A comparative study of three turbulence-closure models for the hydrocyclone problem*. International Journal of Mineral Processing, 77(1): 217–230, doi: 10.1016/j.minpro.2005.06.007.

EASTWICK C.N, SIMMONS K., WANG Y. 2006. *Study of aero-engine oil-air separators*. Journal of Power and Energy, 220(7): 707-717, doi.org/10.1243/09576509JPE116

ERDAL F.M., SHIRAZI S.A., MANTILLA I., SHOHAM O. 1998. *CFD Study of bubble carry-under in gas-liquid cylindrical cyclone separators*. Society of Petroleum Engineers, SPE-49309-M, doi: 10.2118/49309-MS.

ESCUE A., CUI J. 2010. *Comparison of turbulence models in simulating swirling pipe flows*. Applied Mathematical Modelling, 34(10): 2840–2849, doi: 10.1016/j.apm.2009.12.018.

FILIPPONE A., BOJDO N. 2010. *Turboshaft engine air particle separation*. Progress in Aerospace Sciences, 46(5-6): 224, 245, doi.org/10.1016/j.paerosci.2010.02.001.

GAO X., ZHAO Y., YANG X., CHANG Y., PENG X. 2012. *The research on the performance of oil-gas cyclone separators in oil injected compressor systems with considering the collision and breakup of oil droplets*. International Compressor Engineering Conference, p. 2119.

HIRT C.W., NICHOLS B.D. 1981. *Volume of Fluid (VOF) Method for the Dynamics of Free Boundaries*. Journal of Computational Physics, 39: 201–255, doi: 10.1016/0021-9991(81)90145-5.

KRISTOFFERSEN T., HOLDEN C., SKOGESTAD S., EGELAND O. 2017. *Control-Oriented Modelling of Gas-Liquid Cylindrical Cyclones*. American Control Conference, p. 2829–2836, doi: 10.23919/ACC.2017.7963380.

UBBINK O. 1997. *Numerical prediction of two fluid systems with sharp interfaces (Phd)*. Imperial College London, hdl.handle.net/10044/1/8604.

RUDOLF P. 2013. *Simulation of multiphase flow in hydrocyclone*. EPJ Web of Conferences, 45: 01101, doi: 10.1051/epjconf/20134501101.

SZWARC T., WRÓBLEWSKI W., BORZĘCKI T. 2019. *Numerical simulation of cyclone used in aircraft turbine engine*. Modelling in Engineering, 40: 74.

WANG J., MAO Y., LIU M. 2010. *Numerical simulation of strongly swirling flow in cyclone separator by using an advanced RNG k-ε model*. Shiyou Xuebao, Shiyou Jiagong/Acta Petrolei Sinica (Petroleum Processing Section), 26: 8-13.

WANG L., GAO X., FENG J.M., PENG X.Y. 2015. *Research on the two-phase flow and separation mechanism in the oil–gas cyclone separator*. IOP Conf. Series: Materials Science and Engineering, 90: 012075, doi: 10.1088/1757-899X/90/1/012075.

YAKHOT V., ORSZAG S.A. 1986. *Renormalization Group Analysis of Turbulence*. I. *Basic Theory*. Journal of Scientific Computing, 1(1), doi: 10.1007/BF01061452.